Nucleic Acids Research, 1999, Vol. 27, No. 24 **4823–4829**

Efficient aminoacylation of tRNA^{Lys,3} by human lysyl-tRNA synthetase is dependent on covalent continuity between the acceptor stem and the anticodon domain

Timothy Stello, Minh Hong and Karin Musier-Forsyth*

Department of Chemistry, University of Minnesota, 207 Pleasant Street S.E., Minneapolis, MN 55455, USA

Received July 28, 1999; Revised September 15, 1999; Accepted October 25, 1999

ABSTRACT

In this work, we probe the role of the anticodon in tRNA recognition by human lysyl-tRNA synthetase (hLysRS). Large decreases in aminoacylation efficiency are observed upon mutagenesis of anticodon positions U35 and U36 of human tRNA^{Lys,3}. A minihelix derived from the acceptor-TΨC stem–loop domain of human tRNA^{Lys,3} was not specifically aminoacylated by the human enzyme. The presence of an anticodon-derived stem–loop failed to stimulate aminoacylation of the minihelix. Thus, covalent continuity between the acceptor stem and anticodon domains appears to be an important requirement for efficient charging by hLysRS. To further examine the mechanism of communication between the critical anticodon recognition elements and the catalytic site, a two piece semi-synthetic tRNA^{Lys,3} construct was used. The wild-type semi-synthetic tRNA contained a break in the phosphodiester backbone in the D loop and was an efficient substrate for hLysRS. In contrast, a truncated variant that lacked nucleotides 8–17 in the D stem–loop displayed severely reduced catalytic efficiency. The elimination of key tRNA tertiary structural elements has little effect on anticodon-dependent substrate binding but severely impacts formation of the proper transition state for catalysis. Taken together, our studies provide new insights into human tRNA structural requirements for effective transmission of the anticodon recognition signal to the distal acceptor stem domain.

INTRODUCTION

The relationship between aminoacyl-tRNA synthetases and tRNAs establishes the genetic code whereby specific amino acids are esterified to cognate anticodon-bearing tRNAs during translation. All tRNAs have similar secondary and tertiary structures. Synthetase interaction with the cognate tRNA is based on the presence of identity elements within the tRNA that allow for specific binding and catalysis (1). Both the bacterial and yeast recognition systems have been extensively studied. In general, tRNA identity elements are contained primarily within the acceptor stem and anticodon domains (1). These two domains are located at opposite ends of the L-shaped tRNA tertiary structure (2). Precisely how communication between the critical anticodon recognition elements and the catalytic site located ~76 Å away occurs is in general an open question for the synthetases, and undoubtedly involves a complex set of protein–RNA interactions outside the primary recognition sites (1).

Based on both primary sequence and structural data the aminoacyl-tRNA synthetases have been divided into two major classes each containing 10 members (3). The two classes of synthetases have been further organized into distinct subclasses. Class II aminoacyl-tRNA synthetases are characterized by a highly degenerate set of sequence elements known as motifs 1, 2 and 3. The enzymes that belong to subclass IIb (asparaginyl-, aspartyl- and lysyl-tRNA synthetases) are further distinguished by an N-terminal oligonucleotide-binding (OB) fold that recognizes anticodons with uridine at the second position (U35) (4). The specific molecular interactions between this N-terminal domain and the anticodon have been characterized using biochemical and structural methods for yeast aspartyl-tRNA synthetase (AspRS) (5–7) and both *Escherichia coli* and *Thermus thermophilus* lysyl-tRNA synthetases (LysRS) (8–10). Moreover, in the case of *E.coli* LysRS, mutagenesis of anticodon nucleotides 35 and 36 resulted in ≥100-fold decrease in *in vitro* aminoacylation efficiency, whereas mutagenesis of U34 to G had a less dramatic effect (17-fold) on activity (11).

In the case of yeast AspRS, in addition to the anticodon, the acceptor stem contains important recognition elements that are known to make specific contacts with the enzyme (5,7). In particular, mutations at the so-called 'discriminator' base located at position 73 result in decreases in *in vitro* catalytic efficiency that are similar in magnitude to those observed upon anticodon mutagenesis (6). In this system, a minihelix derived from the acceptor stem domain is a substrate for aminoacylation, albeit with a k_{cat} that is reduced ~9000-fold relative to full-length tRNA^{Asp} (12). Attempts to further stimulate minihelix^{Asp} aminoacylation by addition of a separate anticodon stem–loop were unsuccessful (12). Thus, in this subclass IIb yeast system, covalent attachment of the anticodon domain to the acceptor domain appears to be a requirement for effective communication between these two key sites.

In contrast to the yeast AspRS system, previous investigations of another subclass IIb synthetase, namely human LysRS

*To whom correspondence should be addressed. Tel: +1 612 624 0286; Fax: +1 612 626 7541; Email: musier@chem.umn.edu

(hLysRS), showed that it is relatively insensitive to the identity of the discriminator base (13). Based on our knowledge of tRNA recognition by subclass IIb synthetases and bacterial LysRS in particular, we hypothesized that the anticodon nucleotides U35 and U36 would be critical for hLysRS recognition. Moreover, all residues observed to interact with the central U35 base of the anticodon in the known crystal structure of *T.thermophilus* LysRS complexed with $tRNA^{Lys}$ are conserved in the human enzyme (9,13). In the present study, we confirm the importance of the anticodon elements and investigate the mechanism of anticodon-dependent aminoacylation by a human synthetase for the first time. In particular, we elucidate tRNA structural requirements for effective communication between the critical anticodon nucleotides and the catalytic site.

MATERIALS AND METHODS

Protein purification and assays

Two forms of hLysRS were used in this study. Plasmid pM131 encodes an N-terminal truncated form comprising amino acids 66–597 (hLysRS-ΔN65) and was purified from *E.coli* strain pM131/PALΔSΔUTR(DE3) that is also devoid of *E.coli* LysRS activity (13). Although this variant lacks the N-terminal 65 amino acid residues it still contains residues that constitute the entire N-terminal β-barrel OB-fold domain. Plasmid pM368 encodes full-length hLysRS (amino acids 1–597) and an additional N-terminal sequence that includes a His_6 tag (6H-hLysRS) and was purified from protease-deficient *E.coli* strain DE3. The proteins were purified as previously described (13). Enzyme concentrations were estimated by the Bradford method using the Bio-Rad protein assay kit and bovine serum albumin as the standard (14).

Aminoacylation assays using hLysRS were conducted at 30°C as previously reported (13). For wild-type human $tRNA^{Lys,3}$, assays contained 12.5 nM LysRS and tRNA concentrations of 0.25–18 μM. Mutant tRNAs were assayed using 50 nM LysRS and tRNA concentrations of 0.25–7 μM (U36C), 1–12 μM (U35C, U36G and U36A) and 10–25 μM (U35A and U35G). Aminoacylation assays of native human $tRNA^{Lys}$ (partially purified) were carried out using 1.75 nM LysRS and tRNA concentrations of 0.0125–0.25 μM. Native $tRNA^{Lys}$ concentrations were estimated by carrying out plateau-level charging of the tRNA. Two sets of assay conditions were used with the semi-synthetic tRNA construct. When the 17mer and 15mer 5′-oligonucleotides were used, the assays were carried out as for wild-type human $tRNA^{Lys,3}$. The truncated semi-synthetic tRNA constructs prepared with a 5′-14mer, 10mer or 7mer were assayed at 20°C using 50 nM LysRS. The semi-synthetic tRNAs were annealed by mixing a 1.5-fold excess of the 5′-fragment with the 3′-59mer and heating at 60°C for 3 min. $MgCl_2$ was added to 10 mM and the sample was incubated at room temperature for 5 min before placing on ice. The $minihelix^{Lys,3}$ aminoacylation reactions contained 0.125–1.25 μM human LysRS and $minihelix^{Lys,3}$ concentrations varying from 8 to 200 μM. For $minihelix^{Lys,3}$ stimulation attempts an RNA stem–loop mimicking the $tRNA^{Lys,3}$ anticodon domain was added to the aminoacylation reactions at concentrations varying from 20 to 100 μM. Inhibition assays were carried out using 2.5 nM hLysRS and unmodified $tRNA^{Lys,3}$ concentrations of 0.25–8 μM. Concentrations of the inhibitors tested were as follows: 0–8 μM 3′-oxidized $tRNA^{Lys,3}$; 0–60 μM U35G $tRNA^{Lys,3}$; 0–100 μM $minihelix^{Lys,3}$; 0–20 μM UUU anticodon stem–loop; 0–100 μM U35G anticodon stem–loop. Dixon plots were produced and the K_i values were determined from replots of the slopes versus 1/[tRNA] (15).

T7 RNA polymerase was purified according to Grodberg and Dunn (16) from *E.coli* strain BL-21/pAR 1219, which was a gift from Dr F. William Studier.

Ribonucleic acids

Unmodified wild-type human $tRNA^{Lys,3}$ was prepared by *in vitro* transcription from *Fok*I-linearized plasmid pLYSF119 as previously described (13). Mutant $tRNA^{Lys,3}$ variants as well as $minihelix^{Lys,3}$ derived from the acceptor-TΨC stem–loop domain of $tRNA^{Lys,3}$ were prepared by overlap extension PCR mutagenesis (17) and verified by sequencing (18). The gene for 3′-59mer $tRNA^{Lys}$ preceded by a T_7 RNA polymerase promoter was assembled by ligating together six deoxyoligonucleotides as previously described (19). This DNA insert was then ligated into *Eco*RI/*Bam*HI-digested pLYSF119. DEAE-grade human $tRNA^{Lys}$ was purchased from Bio S and T (Montreal, Canada). Synthetic RNA oligonucleotides mimicking the human $tRNA^{Lys,3}$ anticodon stem–loop domain and 5′-regions of the D loop and acceptor stems were prepared by automated solid phase chemical synthesis on a Gene Assembler Plus (Pharmacia) using the phosphoramidite method (20).

To determine concentrations of RNAs at 260 nm the following extinction coefficients were used: 5′-7mer, 6.8×10^4 M^{-1}; 5′-10mer, 8.8×10^4 M^{-1}; 5′-14mer, 11.6×10^4 M^{-1}; 5′-15mer, 12.3×10^4 M^{-1}; 5′-17mer, 13.6×10^4 M^{-1}; anticodon stem–loops (17mer), 13.6×10^4 M^{-1}; $minihelix^{Lys,3}$ (35mer), 26.0×10^4 M^{-1}; 3′-59mer, 42.5×10^4 M^{-1}; full-length tRNAs, 60.4×10^4 M^{-1}.

Native polyacrylamide gel electrophoresis

Native gels consisted of a resolving gel containing 12% acrylamide (29:1 acrylamide:bisacrylamide), 25 mM Tris, 0.12 mM glycine (pH 7.8) and 10 mM $MgCl_2$. The stacking gel contained 5% acrylamide (29:1 acrylamide:bisacrylamide), 25 mM Tris, 0.12 mM glycine (pH 5.8) and 10 mM $MgCl_2$. RNA samples were annealed using the protocols described above and glycerol was added to 25% just before loading. Approximately 7 μg of annealed RNA was applied to each lane. Gels were run at 30 mA for 24 h at room temperature and stained with ethidium bromide for visualization.

RESULTS

We have previously shown that *in vitro* transcripts of human $tRNA^{Lys,3}$ are substrates for both the N-terminal truncated and full-length forms of hLysRS. Both forms of hLysRS were able to efficiently aminoacylate both native and unmodified *E.coli* $tRNA^{Lys}$ indicating that the base modifications are not critical for cross-species aminoacylation (13). In the present study, we used partially purified native human $tRNA^{Lys}$ in aminoacylation assays to examine the effect of base modifications on cognate charging by hLysRS. The k_{cat}/K_m shows a 10-fold decrease for the unmodified transcript compared to the native

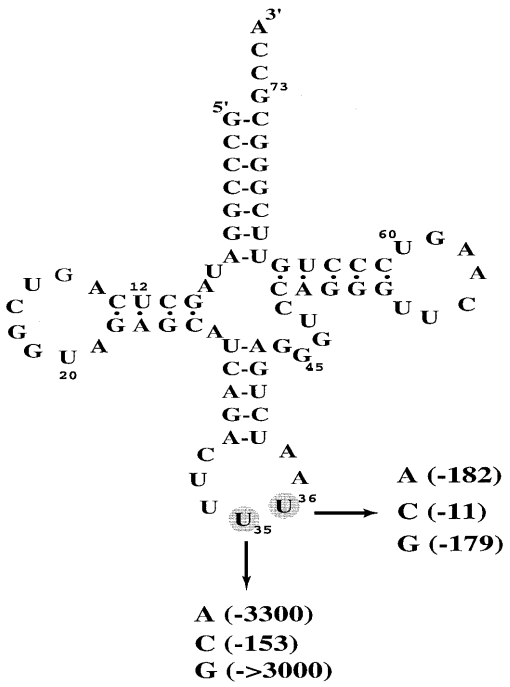

Figure 1. Secondary structure of unmodified human $tRNA^{Lys,3}$ used in this study. The arrows point to individual mutations at positions 35 and 36 that were tested in this work. The numbers represent the fold decrease in k_{cat}/K_m relative to the wild-type unmodified $tRNA^{Lys,3}$.

human $tRNA^{Lys}$, indicating that the base modifications make a modest contribution to recognition of human $tRNA^{Lys}$ by hLysRS.

Anticodon mutations

Figure 1 shows the structure of unmodified human $tRNA^{Lys,3}$ and the individual mutations at the last two positions of the anticodon that were prepared and tested using hLysRS-ΔN65. The results show that mutations at either of these two positions have a significant effect on aminoacylation efficiency, with decreases of 150- to >3000-fold at position 35, and 11- to 180-fold at position 36. The most severe effect was observed upon U35G substitution, which resulted in a complete loss of aminoacylation activity. In general, purine substitutions at both positions resulted in more severe decreases than pyrimidine substitutions (Fig. 1 and Table 1). As shown in Table 1, whereas pyrimidine substitution had little effect on K_m and resulted in moderate decreases in k_{cat}, purine substitutions affected both k_{cat} and K_m. Since no aminoacylation activity was detected for the U35G variant, the effect of this substitution on synthetase binding was examined by carrying out inhibition studies. As shown in Table 2, whereas a 3′-periodate-oxidized $tRNA^{Lys,3}$ variant is an excellent inhibitor of $tRNA^{Lys,3}$ aminoacylation with a K_i of 1.3 μM, the U35G variant has an elevated K_i (42 μM). Thus, this variant is significantly defective in both binding and catalysis.

Although the kinetic parameters reported in Table 1 were determined using the N-terminal truncated form of hLysRS, two of the mutant tRNA variants (U35G and U36G) were tested with the full-length his-tagged enzyme and the results obtained were very similar (data not shown).

Table 1. Kinetic parameters determined from *in vitro* aminoacylation of human $tRNA^{Lys,3}$ variants using hLysRS-ΔN65

$tRNA^{Lys,3}$ variant	k_{cat} (s^{-1})	K_m (μM)	k_{cat}/K_m (relative)	Fold decrease
Wild-type	0.38	3.4	1	
U35A	ND	ND	0.0003	~3000
U35C	0.0079	7.8	0.0065	153
U35G	–	–	–	>3000
U36A	0.0068	9.5	0.0055	182
U36C	0.046	3.7	0.093	11
U35G	0.012	16	0.0056	179

Individual kinetic parameters were derived from Lineweaver–Burk plots and are the average of two or three determinations carried out at 30°C with an average standard deviation of ±52%. ND indicates that the individual kinetic parameters could not be reliably determined because of the high K_m compared to tRNA concentrations routinely used in the assay. No entry indicates there was no detectable activity.

Aminoacylation of minihelix^{Lys,3}

Acceptor-TΨC stem–loop-derived minihelices are substrates for many aminoacyl-tRNA synthetases despite the fact that they lack the anticodon and D stem–loop domains (21). Even in cases where the anticodon is a major recognition element, minihelices have been shown to be specifically aminoacylated. However, very few human synthetases have been tested for minihelix aminoacylation to date. We prepared the minihelix corresponding to the acceptor-TΨC stem–loop domain of human $tRNA^{Lys,3}$ (Fig. 2) and tested it in aminoacylation assays with hLysRS. The minihelix was not detectably aminoacylated by the human enzyme even when high concentrations of RNA (200 μM) and hLysRS (1 μM) were included in the assay. The minihelix weakly inhibited aminoacylation of $tRNA^{Lys,3}$ (data not shown). Based on inhibition experiments we estimate that the K_i is ≥100 μM; however, due to the relatively weak binding, it was only possible to determine a lower limit for the K_i value. Thus, the lack of charging even at high minihelix concentrations may, in part, be attributed to a lower binding affinity.

We next determined whether the addition of an RNA stem–loop mimicking the anticodon domain of $tRNA^{Lys,3}$ (Fig. 2) could stimulate minihelix^{Lys,3} aminoacylation. We first established that the wild-type anticodon was a good inhibitor of $tRNA^{Lys,3}$ aminoacylation, with a K_i of 5 μM (Table 2), indicating that binding to LysRS was similar to the full-length tRNA. Moreover, the specificity of anticodon binding is maintained in the context of the RNA stem–loop, since a U35G anticodon stem–loop variant is a significantly weaker inhibitor with a K_i of 33 μM (Table 2). Nevertheless, we were unable to observe any detectable minihelix^{Lys,3} aminoacylation even upon addition of 100 μM anticodon stem–loop domain.

Aminoacylation of semi-synthetic $tRNA^{Lys,3}$

Aminoacylation experiments with the minihelix^{Lys,3} and anticodon stem–loops suggest that covalent continuity is required for communication between the critical anticodon elements and the site of aminoacylation. To elucidate whether the entire tRNA structure is required for the anticodon to trigger aminoacylation of the acceptor stem domain, semi-synthetic tRNA constructs were prepared. The first semi-synthetic

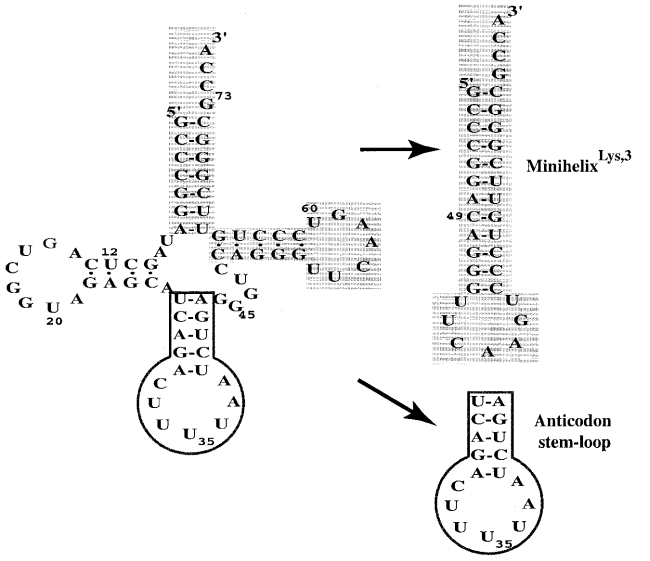

Figure 2. Structure of stem–loop domains derived from human $tRNA^{Lys,3}$ used in this work. The anticodon stem–loop domain (boxed) was chemically synthesized while the acceptor-TΨC stem–loop $minihelix^{Lys,3}$ (shaded) was prepared by *in vitro* transcription.

construct tested contained a break in the sugar–phosphate backbone between nucleotides 17 and 18 of the D loop (Fig. 3). A similar construct was shown to be active in the *E.coli* ProRS system (22). Aminoacylation assays with hLysRS showed that this semi-synthetic $tRNA^{Lys,3}$ (3′-59mer + 5′-17mer) was indeed an efficient substrate, with a k_{cat}/K_m within a factor of 2 of the wild-type tRNA (Table 3 and Fig. 4). In contrast, the 3′-59mer alone (Fig. 3, top right), which contains the CCA 3′-end, was not aminoacylated by the synthetase (Fig. 4). A second semi-synthetic tRNA was prepared using only a 5′-7mer oligomer annealed to the 3′-59mer (Fig. 3). This construct maintains covalent continuity between the acceptor stem and anticodon domains but disrupts the tRNA tertiary core structure by deletion of nucleotides 8–17. This construct was a very poor substrate for the synthetase with a k_{cat}/K_m that was 2700-fold reduced relative to the intact tRNA (Table 3 and Fig. 4). Comparison of the individual kinetic parameters shows that the decreased efficiency of the truncated semi-synthetic construct is primarily due to a 6500-fold decrease in k_{cat}, while the K_m is 2-fold lower (Table 3). Upon introduction of the U35G mutation into the 3′-59mer fragment the aminoacylation activity of both semi-synthetic tRNA constructs was eliminated (data not shown). Thus, despite maintenance of anticodon binding specificity, the truncated semi-synthetic construct was severely defective in formation of the transition state for catalysis.

To more precisely determine the structural elements that contribute to the k_{cat} defect in the truncated semi-synthetic tRNA, three additional constructs were tested (Fig. 3). In all cases, a truncated 5′-oligomer was annealed to the 3′-59mer. When a 5′-15mer was used, wild-type levels of aminoacylation were observed (Fig. 4). In contrast, deletion of one more nucleotide from the 3′-end (5′-14mer) resulted in a significant decrease in catalytic efficiency (Fig. 4). This semi-synthetic tRNA lacks the capability to make a key tertiary contact, namely the G15:C48 Levitt base pair (23). A more careful kinetic analysis of this variant showed that the defect was due to an ~2-fold reduction in k_{cat} and a 3-fold elevation in K_m (Table 3). Finally, truncation to a 5′-10mer resulted in even lower levels of activity, similar to the 5′-7mer construct (Fig. 4).

Table 2. Inhibition constants determined from *in vitro* aminoacylation of unmodified human $tRNA^{Lys,3}$ using 6H-hLysRS

Inhibitor	K_i (μM)
$tRNA^{Lys,3}$ (3′-oxidized)	1.3
$tRNA^{Lys,3}$ (U35G)	42
Anticodon stem–loop (WT)	5
Anticodon stem–loop (U35G)	33

K_i values are the average of two determinations and were derived from Dixon plot analysis of the initial rate data (Materials and Methods). All assays were carried out at 30°C. The two trials differed by ≤25%.

To determine if the 5′-oligonucleotides were annealing to the 3′-59mer in the semi-synthetic constructs, migration of the annealed tRNA molecules on a native polyacrylamide gel run at room temperature was compared to that of the full-length $tRNA^{Lys,3}$. The native gel shown in Figure 5 compares the mobility of full-length $tRNA^{Lys,3}$ (lane 1, arrow), the 3′-59mer alone (lane 2), and the five annealed semi-synthetic tRNA constructs (lanes 3–7). The 3′-59mer (lane 2) migrates as several smeared bands, presumably due to conformational flexibility, with the major band migrating significantly slower than the full-length tRNA (lane 1). Each of the annealed semi-synthetic tRNAs (lanes 3–7) migrates as a single compact band and to a similar distance as the full-length tRNA. These results suggest that the semi-synthetic constructs are properly annealed and fold into a conformation that closely resembles that of the full-length tRNA molecule.

DISCUSSION

A previous *in vitro* study of *E.coli* $tRNA^{Lys}$ recognition found that *E.coli* LysRS required the discriminator base and the anticodon for efficient aminoacylation (11). Moreover, a 140-fold difference in catalytic efficiency was observed between unmodified and fully modified *E.coli* $tRNA^{Lys}$. Multiple alignments of 21 class II LysRS sequences previously indicated that the catalytic domain is one of the most highly conserved domains among synthetases (13). Nevertheless, in contrast to the *E.coli* enzyme, our earlier *in vitro* work with hLysRS showed it to be insensitive to the identity of the discriminator base (13). The fact that the human enzyme could efficiently aminoacylate both native and unmodified *E.coli* $tRNA^{Lys}$ also suggested that this enzyme is relatively insensitive to base modifications. The human $tRNA^{Lys,3}$ isoacceptor is extensively modified, containing 13 base modifications. In this work, using a crude preparation of native human $tRNA^{Lys}$, we observed only a 10-fold contribution of base modifications to aminoacylation catalytic efficiency of hLysRS. Thus, modified bases are not essential for hLysRS recognition, but contribute modestly to overall catalytic efficiency.

In this study, we also probed anticodon recognition by hLysRS. It is well established that the subclass IIb synthetases recognize the anticodon via an N-terminal OB-fold domain (4).

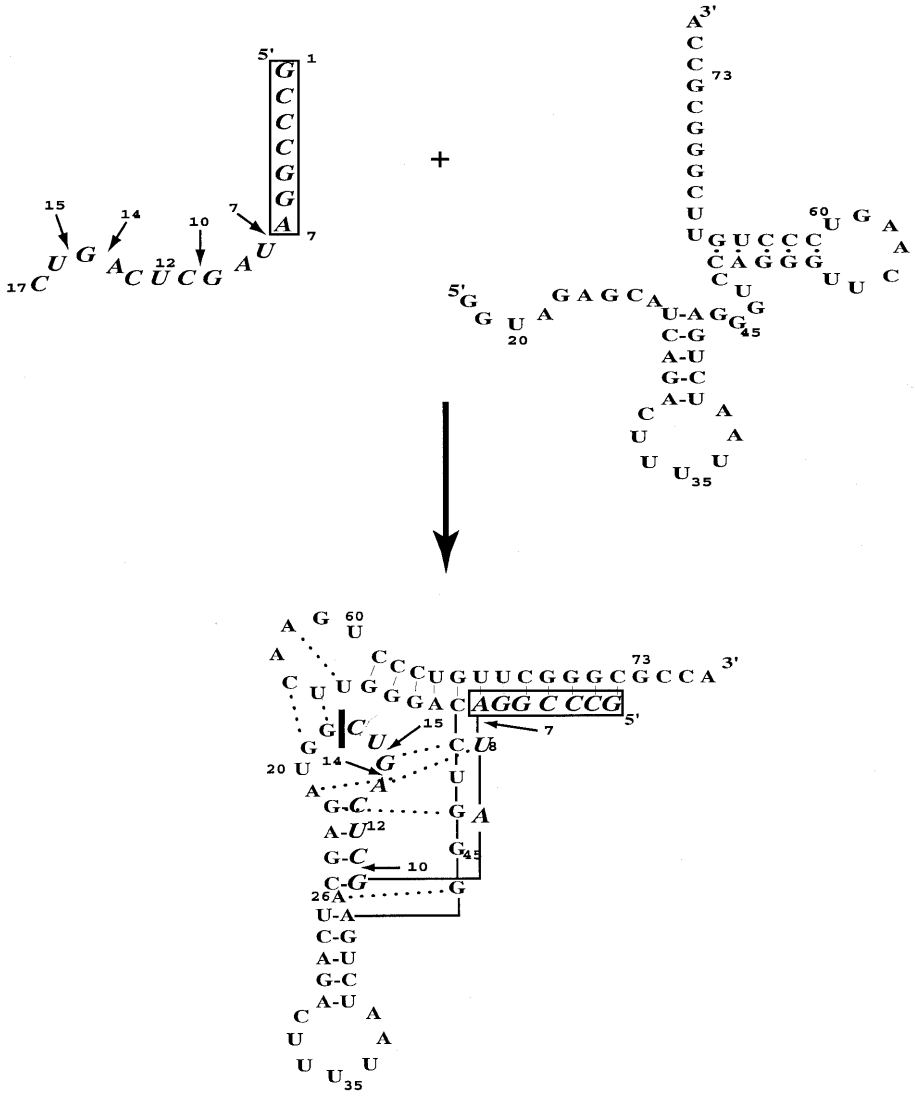

Figure 3. Scheme showing preparation of semi-synthetic tRNAs. A chemically synthesized 5′-oligonucleotide (17mer, indicated in larger font and italics) is annealed to an *in vitro* transcribed 3′-59mer fragment. The solid black line in the folded L-shaped representation indicates a break in the sugar–phosphate backbone in the wild-type construct prepared with the 5′-17mer. The truncated semi-synthetic variants are shown by numbered arrows indicating the length of each fragment from the 5′-end. The 5′-7mer is also boxed. Dotted lines in the L-shaped representation indicate tertiary interactions and are based on the known structure of yeast $tRNA^{Phe}$ (2).

Table 3. Kinetic parameters determined from *in vitro* aminoacylation of full-length and semi-synthetic $tRNA^{Lys,3}$ using 6H-hLysRS

$tRNA^{Lys,3}$variant	Temperature (°C)	k_{cat} (s^{-1})	K_m (μM)	k_{cat}/K_m (relative)	Fold decrease
Wild-type	30	2.0	3.4	1	
	20	1.7	3.7	1	
3′-59mer					
+ 5′-17mer	30	1.5	5.1	0.63	1.6
+ 5′-14mer	20	0.88	8.9	0.22	4.5
+ 5′-7mer	20	0.00026	1.5	0.00037	2700

Individual kinetic parameters were derived from Lineweaver–Burk plots and are the average of two or three determinations with an average standard deviation of ±50%. For the 3′-59mer + 5′-14mer or 5′-7mer optimal activity in the aminoacylation assay was observed at 20°C. The aminoacylation efficiencies of these two constructs are thus reported relative to the wild-type (full-length) $tRNA^{Lys,3}$, which was also assayed at this temperature.

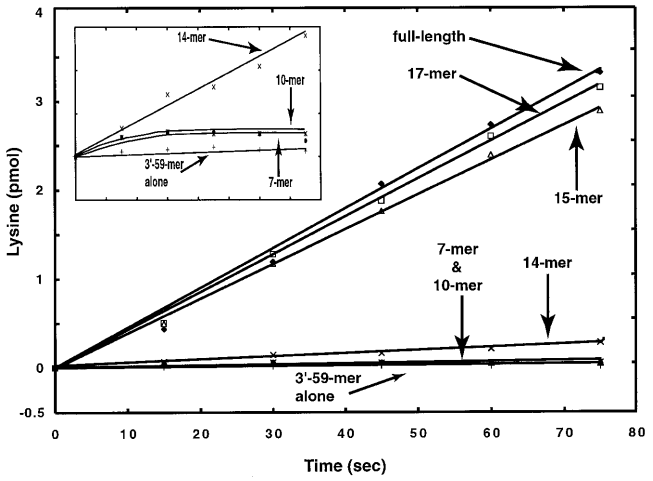

Figure 4. Comparison of aminoacylation activity of full-length unmodified $tRNA^{Lys,3}$ and semi-synthetic tRNA constructs. The semi-synthetic tRNAs are indicated by the length of the 5′-oligonucleotide. The inset shows an expanded view of the results obtained with the shorter constructs. All RNAs were assayed at 5 μM, with the exception of the 3′-59mer alone, which was present at 2 μM.

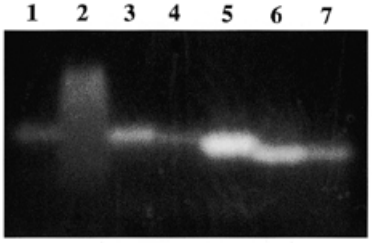

Figure 5. Ethidium stained, native 12% polyacrylamide gel showing: full-length $tRNA^{Lys,3}$ (lane 1); 3′-59mer alone (lane 2); 3′-59mer + 5′-17mer (lane 3); + 5′-15mer (lane 4); + 5′-14mer (lane 5); + 5′-10mer (lane 6); + 5′-7mer (lane 7).

The N-terminal anticodon binding domain shows only moderate sequence conservation (8%) among the 21 LysRS sequences previously examined (13). Our results show that the effect of mutations at U36 of human $tRNA^{Lys,3}$ was similar to the decreases in aminoacylation observed in the *E.coli* $tRNA^{Lys}$ system (11). On the other hand, mutagenesis of U35 to G or A has a larger effect on aminoacylation in the human system than in the *E.coli* system. To date, no major recognition elements have been identified in the acceptor stem of human $tRNA^{Lys,3}$, and our results suggest that the eukaryotic system has an even greater anticodon dependence than the prokaryotic system.

In the three-dimensional L-shaped tRNA structure, the site of aminoacylation and the anticodon are ~76 Å apart (2). The mechanistic details of how communication is achieved between the anticodon and the amino acid attachment site are not well understood for most aminoacylation systems, and a complex set of RNA–protein interactions are likely to be involved. To gain some insights into this question, attempts have been made in some systems to stimulate charging of an acceptor stem-derived minihelix with the anticodon stem–loop domain. Most of this work has been carried out using class I synthetases from *E.coli* or yeast (24–28). For two of the systems studied, *E.coli* isoleucyl-tRNA synthetase and yeast valyl-tRNA synthetase, small increases (2–3-fold) in minihelix aminoacylation were observed upon anticodon addition (24,28). The yeast AspRS system is the only subclass IIb system where minihelix aminoacylation has been reported (12). Although $minihelix^{Asp}$ alone is aminoacylated by yeast AspRS, a stem–loop mimicking the anticodon of $tRNA^{Asp}$ was not capable of stimulating the aminoacylation further (12).

In our experiments with the human lysine system, we find that a minihelix derived from the acceptor-TΨC stem–loop of human $tRNA^{Lys,3}$ is not charged and that the anticodon stem–loop fails to trigger $minihelix^{Lys,3}$ aminoacylation. These data suggest that covalent continuity between these two key elements is required for aminoacylation by hLysRS. In support of the notion that covalent continuity is sufficient for at least low levels of aminoacylation in the lysine system, yeast and rabbit liver LysRS were reported to weakly aminoacylate a substrate consisting of 5′-G(U_{20})CCA-3′ (29). In the case of the yeast enzyme, which displayed higher activity than the rabbit enzyme in these previous studies, the 3′-U in the single-stranded substrate may mimic N73 of the full-length yeast $tRNA^{Lys}$ and the 5′-region of the oligomer may mimic the UUU anticodon. This result suggests that simply by maintaining covalent continuity between the two distal elements, the lysine anticodon trinucleotide is able to trigger acceptor stem aminoacylation.

To probe this idea further, we have dissected human $tRNA^{Lys,3}$ in more subtle ways and carried out a kinetic analysis of semi-synthetic tRNA variants (Fig. 3 and Table 3). Simply introducing a break in the sugar–phosphate backbone after C17 does not significantly affect aminoacylation catalytic efficiency. However, when sequence elements in the D stem–loop known to be involved in core tRNA tertiary interactions are deleted, hLysRS catalytic efficiency is severely affected despite the fact that the global tRNA-like fold is maintained (Fig. 5). Most strikingly, the 2700-fold decrease in catalytic efficiency observed with the 3′-59mer + 5′-7mer construct was entirely due to a decrease in k_{cat}, with binding actually slightly improved relative to the full-length tRNA (Table 3). Thus, the anticodon domain of this semi-synthetic tRNA construct is likely to be properly bound to the synthetase. Specificity of the binding interaction is supported by the fact that a U35→G substitution in the semi-synthetic construct abolishes activity. The inhibition trends observed with stem–loops bearing UUU and UGU anticodon sequences also suggest that hLysRS is able to specifically recognize the major (U35) recognition element in the context of a simple RNA stem–loop (Table 2). Thus, the primary effect of deleting key tertiary structural elements is on the transition state of the aminoacylation reaction. The similarity in K_i values determined for both full-length and truncated U35G variants is in accord with the critical nature of the interactions between the central anticodon base and the N-terminal OB-fold (9).

The presence of D stem elements and tRNA tertiary structure was also shown to be important for aminoacylation by class I yeast methionyl-tRNA synthetase, although whether deletion of the D arm affected primarily k_{cat} or K_m was not reported in this study (26). These researchers concluded that although most of the binding energy is localized in the anticodon region, protein contacts with the D arm are required for optimal

catalysis. In the case of another class I enzyme, *E.coli* glutaminyl-tRNA synthetase, specific amino acids that interact with the inside of the L-shaped tRNA have been identified. This is one of the few systems where a high resolution co-crystal structure of the synthetase complexed with tRNA is known (30). Synthetase mutations at these interaction sites result in relaxed anticodon recognition, thus providing a connection between the acceptor end and the anticodon domain (31).

Subclass IIb yeast AspRS is one of two class II enzymes for which high a resolution X-ray structure in complex with the tRNA has been reported (5). In this case, the acceptor stem contains key recognition elements (of approximately equal importance to the anticodon) and a minihelix is aminoacylated by yeast AspRS. The addition of a separate anticodon domain was not able to stimulate catalysis, presumably due to missing RNA–protein contacts present in the intact L-shaped structure (12). Based on the co-crystal structure, enzyme contacts to backbone functional groups of U11 and U12 in the D stem are observed (7). However, mutations at a neighboring identity element, the G10:U25 base pair, affect primarily the K_m (6), and it is not clear whether these contacts are needed to communicate anticodon recognition to the active site. In the human lysine system studied here, we have shown that the anticodon makes a much larger relative contribution to aminoacylation catalytic efficiency than the acceptor stem. Based on this observation, it is not too surprising that minihelix^{Lys,3} is not aminoacylated by hLysRS. We show that effective communication of the anticodon binding energy to the active site requires the presence of a relatively small number of key tertiary structural elements. More specifically, the presence of an intact Levitt base pair (G15:C48) contributes 0.88 kcal/mol to the apparent free energy of transition state stabilization, while nucleotides 8–14 in the D arm contribute an additional 4.6 kcal/mol.

In summary, in this work we show that the anticodon is a critical recognition element for hLysRS and examine the mechanism of communication between the anticodon and the amino acid acceptor stem domain in a human system for the first time. As reported previously for several *E.coli* and yeast aminoacylation systems, covalent continuity between the acceptor and anticodon domains appears to be an important requirement for efficient charging by the human synthetase. Elimination of tertiary structural elements of tRNA^{Lys,3} has little effect on anticodon-dependent substrate binding, but severely impacts formation of the transition state for catalysis. Taken together, our results suggest that a relatively small number of specific tertiary structural elements of human tRNA^{Lys,3} are responsible for conferring effective communication between the crucial anticodon recognition elements and the acceptor stem.

REFERENCES

1. Giegé,R., Sissler,M. and Florentz,C. (1998) *Nucleic Acids Res.*, **26**, 5017–5035.
2. Kim,S.H., Suddath,F.L., Quigley,G.J., McPherson,A., Sussman,J.L., Wang,A.H.J., Seeman,N.C. and Rich,A. (1974) *Science*, **185**, 435–440.
3. Eriani,G., Delarue,M., Poch,O., Gangloff,J. and Moras,D. (1990) *Nature*, **347**, 203–206.
4. Cusack,S., Yaremchuk,A. and Tukalo,M. (1997) In Eggleston,D.S. (ed.), *The Many Faces of RNA*. Academic Press, San Diego, CA, pp. 55–64.
5. Ruff,M., Krishnaswamy,S., Boeglin,M., Poterszman,A., Mitschler,A., Podjarny,A., Rees,B., Thierry,J.C. and Moras,D. (1991) *Science*, **252**, 1682–1689.
6. Pütz,J., Puglisi,J.D., Florentz,C. and Giegé,R. (1991) *Science*, **252**, 1696–1699.
7. Cavarelli,J., Rees,B., Ruff,M., Thierry,J.-C. and Moras,D. (1993) *Nature*, **362**, 181–184.
8. Commans,S., Plateau,P., Blanquet,S. and Dardel,F. (1995) *J. Mol. Biol.*, **253**, 100–113.
9. Cusack,S., Yaremchuk,A. and Tukalo,M. (1996) *EMBO J.*, **15**, 6321–6334.
10. Commans,S., Lazard,M., Delort,F., Blanquet,S. and Plateau,P. (1998) *J. Mol. Biol.*, **278**, 801–813.
11. Tamura,K., Himeno,H., Asahara,H., Hasegawa,T. and Shimizu,M. (1992) *Nucleic Acids Res.*, **20**, 2335–2339.
12. Frugier,M., Florentz,C. and Giegé,R. (1994) *EMBO J.*, **13**, 2218–2226.
13. Shiba,K., Stello,T., Motegi,H., Noda,T., Musier-Forsyth,K. and Schimmel,P. (1997) *J. Biol. Chem.*, **272**, 22809–22816.
14. Bradford,M.M. (1976) *Anal. Biochem.*, **72**, 248–254.
15. Segel,I.H. (1975) *Enzyme Kinetics*. John Wiley & Sons, New York, NY.
16. Grodberg,J.D. and Dunn,J.J. (1988) *J. Bacteriol.*, **170**, 1245–1253.
17. Horton,R.M. and Pease,L.R. (1991) In McPherson,M.J. (ed.), *Directed Mutagenesis*. IRL Press, New York, NY, pp. 217–247.
18. Sanger,F., Nicklen,S. and Coulson,A.R. (1977) *Proc. Natl Acad. Sci. USA*, **74**, 5463–5467.
19. Sampson,J.R. and Uhlenbeck,O.C. (1988) *Proc. Natl Acad. Sci. USA*, **85**, 1033–1037.
20. Scaringe,S.A., Francklyn,C. and Usman,N. (1990) *Nucleic Acids Res.*, **18**, 5433–5441.
21. Musier-Forsyth,K. and Schimmel,P. (1999) *Acc. Chem. Res.*, **32**, 368–375.
22. Liu,H. and Musier-Forsyth,K. (1994) *Biochemistry*, **33**, 12708–12714.
23. Levitt,M. (1969) *Nature*, **224**, 759–763.
24. Frugier,M., Florentz,C. and Giegé,R. (1992) *Proc. Natl Acad. Sci. USA*, **89**, 3990–3994.
25. Wright,D., Martinis,S., Jahn,M., Söll,D. and Schimmel,P. (1993) *Biochimie*, **75**, 1041–1049.
26. Senger,B., Aphasizhev,R., Walter,P. and Fasiolo,F. (1995) *J. Mol. Biol.*, **249**, 45–58.
27. Hamann,C.S. and Hou,Y.-M. (1995) *Biochemistry*, **34**, 6527–6532.
28. Nureki,O., Niimi,T., Muto,Y., Kanno,H., Kohno,T., Muramatsu,T., Kawai,G., Miyazawa,T., Giegé,R., Florentz,C. and Yokoyama,S. (1993) In Nierhaus,K., Fransceschi,F., Subramanian,A., Erdmann,V. and Wittmann-Liebold,B. (eds), *The Translation Apparatus*. Plenum Press, New York, NY, pp. 59–66.
29. Khvorova,A.M., Motorin,Y.A., Wolfson,A.D. and Gladilin,K.L. (1992) *FEBS Lett.*, **314**, 256–258.
30. Rould,M.A., Perona,J.J., Söll,D. and Steitz,T.A. (1989) *Science*, **246**, 1135–1142.
31. Rogers,M.J., Adachi,T., Inokuchi,H. and Söll,D. (1994) *Proc. Natl Acad. Sci. USA*, **91**, 291–295.